JTTEE 3:135-141

Low-Pressure Plasma Deposition of Tungsten

W. Cai, H. Liu, A. Sickinger, E. Muehlberger, D. Bailey, and E.J. Lavernia

This study investigated the microstructure of tungsten produced by the low-pressure plasma spraying (LPPS) process, with particular attention given to the mechanisms that govern the formation of porosity. Accordingly, contamination in the LPPS-processed tungsten was evaluated by measuring the carbon, oxygen, and nitrogen contents. The LPPS-processed tungsten contained 100 ppm C, 26 ppm N_2, and 154 ppm O_2, compared to 10, 12, and 250 ppm, respectively, in the as-received powder. X-ray diffractometry studies failed to reveal the presence of any reaction products in the LPPS-processed tungsten. Regarding porosity, studies using scanning electron microscopy revealed that an elevated concentration of micrometer-sized pores was present in the LPPS-processed tungsten. The mechanisms governing the formation of porosity are discussed in terms of the following four factors: the presence of the unmelted powders in the deposit, the interaction between droplets and deposition surface, the presence of porosity in the as-received powder, and the formation of solidification shrinkage.

1. Introduction

ITS unique combination of physical properties renders tungsten one of the most important metals for high-temperature applications. Tungsten has the highest melting point (3387 °C) of all metallic elements and an exceptionally high density (19.25 g/cm^3) (Ref 1). In addition, tungsten exhibits an unusually high elastic modulus (414 GPa) and is the only metal that possesses elastic isotropy (Ref 2). As a result of these physical attributes, tungsten has been widely used in commercial lamp filaments, aerospace propulsion, energy production, and many other applications (Ref 2, 3). Moreover, tungsten is an important alloying element in tool steels and superalloys (Ref 2).

The high melting point, low oxidation resistance, and poor workability of tungsten and tungsten alloys have prompted the study and application of near-net-shape processes as potential approaches to fabrication of these materials. As a result of these efforts, a variety of techniques have been successfully developed for the processing of tungsten and tungsten alloys, including solid-state sintering and mechanical working (Ref 2-4), liquid-phase sintering (Ref 2, 3), chemical vapor deposition (Ref 2, 4), arc casting (Ref 2, 4), electron beam melting (Ref 2), and plasma spraying (Ref 4, 5). Among these, plasma spraying is a promising near-net-shape technique that combines melting, quenching, and consolidation into a single operation and produces very fine-grained and homogeneous microstructures (Ref 6-9).

The application of plasma spraying for the production of intricate shapes of tungsten can be traced back to the 1960s, when a tungsten expansion nozzle and a tungsten crucible were produced by plasma spraying (Ref 5). Among the various available plasma-spraying techniques, low-pressure plasma spraying (LPPS) appears to yield the most promising results for a variety of materials, such as metallic alloys, intermetallics, ceramics, and composites (Ref 9). It recently has been reported that tungsten structures can be readily fabricated using LPPS. These structures include tungsten rocket nozzles (Ref 9) and tungsten pipes with internal threads (Ref 10). Moreover, the interest in LPPS-processed tungsten also encompasses alloys, such as W-Ni-Fe (Ref 11). However, several issues must be resolved before optimal microstructure and properties can be achieved in LPPS-processed tungsten. Jackson et al. (Ref 12), for example, note that incomplete melting of coarse tungsten powders leads to excessive porosity in LPPS-processed tungsten.

The present study was undertaken to provide preliminary information on the evolution of microstructure during LPPS processing of tungsten. To accomplish this objective, a LPPS experiment was conducted, and a 2 to 3 mm thick tungsten deposit was prepared. The microstructure of the LPPS-processed tungsten was then characterized in detail, with particular attention given to the presence of porosity and contamination by oxygen, nitrogen, and carbon. Finally, the mechanisms that govern the formation of porosity during LPPS were discussed in light of experimental and numerical results.

Key Words: low-pressure plasma spraying, microstructure, porosity, tungsten deposition

W. Cai, H. Liu, and **E. J. Lavernia,** Materials Science and Engineering, Department of Mechanical and Aerospace Engineering, University of California, Irvine, CA 92717, USA; **A. Sickinger, E. Muehlberger,** and **D. Bailey,** Electro-Plasma, Inc., Irvine, CA 92714, USA

2. Experimental Procedure

The plasma spraying of tungsten was conducted at Electro-Plasma Inc. (Irvine, CA) using an EPI-LPPS^{TM} Electro-Plasma Inc. (Irvine, CA) system and an EPI-03CP plasma gun. First, a thin molybdenum coating (about 0.2 mm thick) was plasma sprayed on a cylindrical graphite substrate. The objective of this step was to form a diffusion barrier between tungsten and graphite and thus to prevent the formation of tungsten carbide in the deposit. Second, pure tungsten powders (purity, ~99.9%; size, –45 + 15 μm) were plasma sprayed and deposited on the molybdenum-coated graphite substrate, using the following primary processing parameters:

Power, kW	135
Plasma gas ratio: Ar/H_2	10:1
Powder feed rate, g/min	75
Spray distance, mm	250
Atmosphere, torr	80

The substrate was heated to a temperature of 1500 °C before and after plasma spraying.

Following LPPS processing, the as-deposited tungsten (about 2 to 3 mm thick) was sectioned, polished, and etched using modified Murakami's reagent, which contained 15 g $K_3Fe(CH)_6$, 2 g NaOH, and 100 mL H_2O. The microstructure was then studied using optical microscopy. The average grain size and size distribution were determined using a computer-assisted image analysis facility.

To determine the density of the deposited materials, the molybdenum layer and the interaction zone (approximately 125 μm thick) that formed between molybdenum and tungsten were dissolved using a solution of 2% H_2O_2. The density of the deposited tungsten was then determined on the basis of Archimedes' principle. Scanning electron microscopy (SEM) with a Hitachi S-500 instrument was used to document the morphology and location of pores in the deposited tungsten. Furthermore, to provide insight into the mechanisms that govern the formation of porosity during LPPS, the as-received tungsten powders were examined using SEM.

To evaluate the extent of contamination during LPPS, the levels of carbon, nitrogen, and oxygen in the deposit were measured.* In addition, to determine the possible presence of compounds that may have formed during plasma spraying, x-ray diffraction (XRD) studies were conducted on the LPPS-processed tungsten using a Siemens D-5000 diffractometer.

3. Results and Discussion

3.1 *Microstructure of LPPS-Processed Tungsten*

The microstructure of the LPPS-processed tungsten is shown in Fig. 1. The deposited material exhibited an equiaxed grain morphology, with grain sizes varying from 3 to 90 μm and an average size of 17 μm (Fig. 2). Moreover, inspection of the grain morphology reveals that recrystallization occurred during deposition. This microstructure is different from the lamellae or wavy microstructures that are typically exhibited by other as-plasma-sprayed materials, such as Ni_3Al and nickel-base alloys (Ref 8, 13). Upon annealing, however, the microstructures of these materials become similar to that presently observed for tungsten, indicating that the tungsten experienced exposure to elevated temperature during plasma spraying. Actually, deliberate heating of the substrate following spraying can be viewed as an annealing process. This practice is generally used during the plasma spraying of refractory metals to control residual stress and to increase density, as reported by Smith and Apelian (Ref 13). Moreover, the interaction between the plasma and the substrate, as well as the release of the latent heat of fusion ($H_f = 1.71426 \times 10^5$ J/kg for tungsten, Ref 14), further enhances recrystallization and grain growth in the deposited materials (Ref 8).

It is well established that LPPS is a rapid-solidification process capable of reaching a cooling rate greater than 10^4 K/s (Ref 7, 13), which should result in a very fine-grained morphology. For example, it has been reported that as-plasma-deposited tantalum and niobium exhibited grain sizes ranging from 0.1 to 0.5 μm (Ref 15). However, the grain size observed herein is relatively large (3 to 90 μm), providing further support to the suggestion that recrystallization and grain growth occur during plasma spraying processes. Therefore, further optimization of the operating parameters may

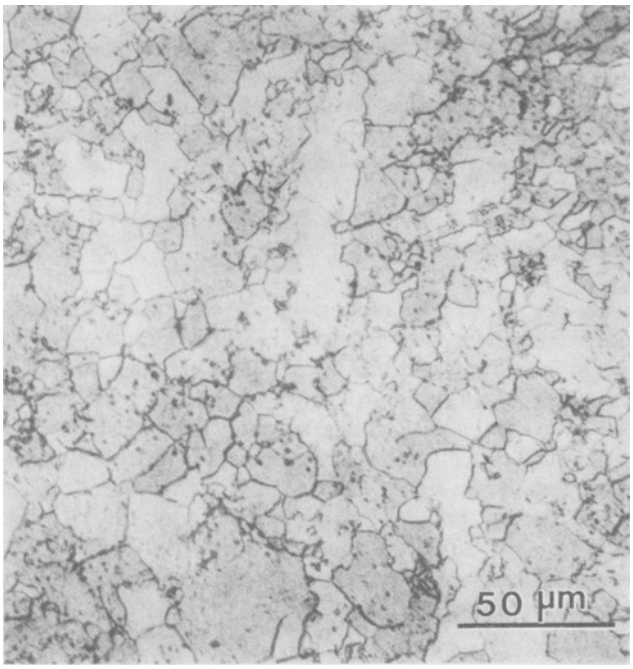

Fig. 1 Microstructure of the LPPS-processed tungsten. Etched with modified Murakami's reagent

*The analysis was done by Hermann C. Starck, Berlin, Germany.

Table 1 Comparison of carbon and gas contents before and after plasma spraying

Element	Tungsten powder, ppm	Tungsten deposit, ppm
Carbon	10	100
Nitrogen	12	26
Oxygen	250	154

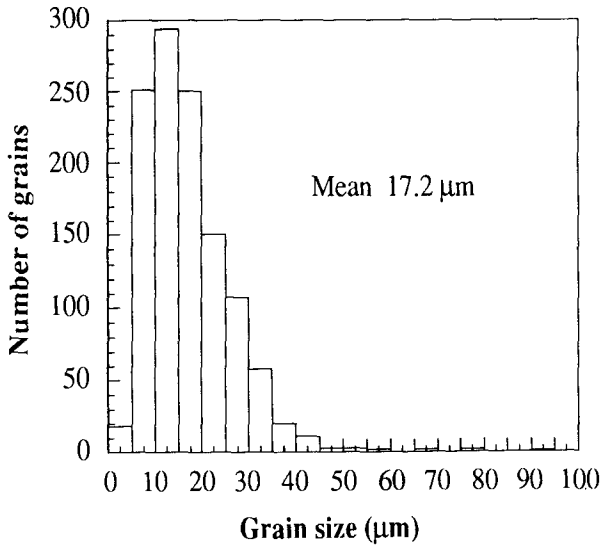

Fig. 2 Distribution of grain sizes obtained from computerized image analysis

be necessary if LPPS is used to obtain a highly refined microstructure. Work in this area continues.

3.2 *Contamination of LPPS-Processed Tungsten*

Tungsten, like all refractory metals, is very sensitive to carbon, nitrogen, and oxygen contamination (Ref 16). Accordingly, it is important to minimize contamination during plasma spraying. The concentrations of carbon, nitrogen, and oxygen in the as-received tungsten powders and the LPPS-processed tungsten were measured, and the results are summarized in Table 1. The carbon content increased from 10 ppm to 100 ppm following LPPS processing. The use of a graphite substrate is thought to be responsible for the increase in carbon content. During plasma processing, free carbon escapes from the graphite substrate into the chamber atmosphere, becomes entrapped in the spray stream, and finally leads to the increase in carbon content in the LPPS-processed tungsten. The nitrogen content was found to increase slightly from 12 ppm to 26 ppm (Table 1). Nevertheless, the absolute contents of carbon and nitrogen in the plasma-deposited material were relatively low, suggesting that contamination by carbon and nitrogen is not a severe problem. On the other hand, the oxygen content decreased from 250 ppm to 154 ppm following LPPS processing. Similar observations have been reported for plasma-deposited niobium and its alloys, and it has been suggested that the decrease in oxygen content may be attributable to the removal of oxygen from the powder surface due to volatilization of the powder during spraying (Ref 12). This mechanism may also explain the decrease in oxygen contents observed herein. To that effect, it is well established that WO_3 is volatile above 800 °C (Ref 17); therefore, it is highly probable that any WO_3 that may have been present on the surface of the tungsten powders was vaporized during plasma spraying, thereby leading to a decrease in the oxygen content. Evidently, LPPS effectively prevents the oxidation of tungsten, thus overcoming one of the major drawbacks associated with conventional plasma spraying (Ref 6).

To determine the possible presence of compounds that may have formed during plasma spraying, XRD studies were conducted on the LPPS-processed tungsten. These studies failed to

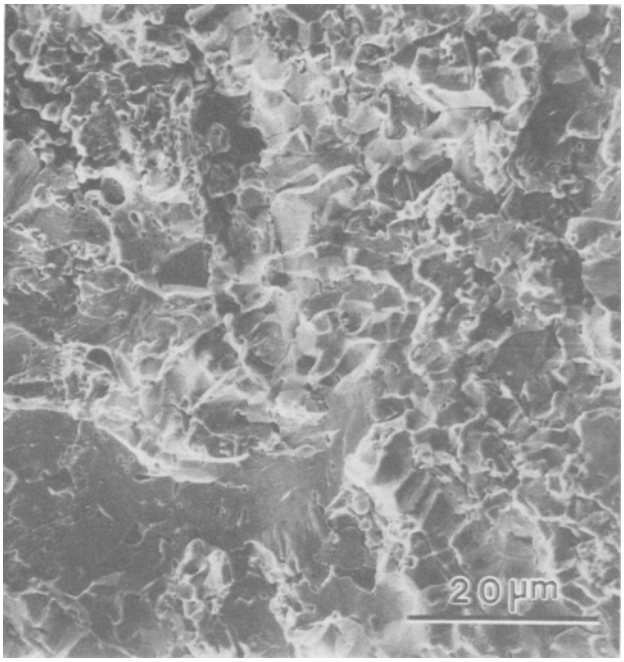

(a)

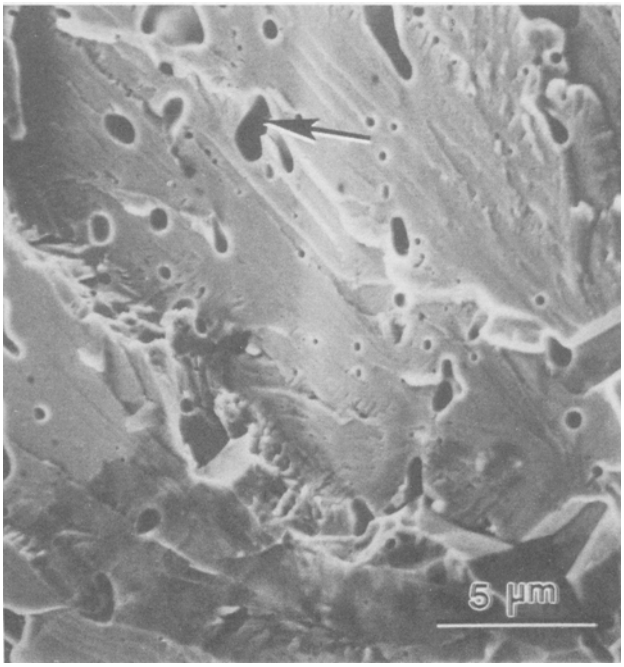

(b)

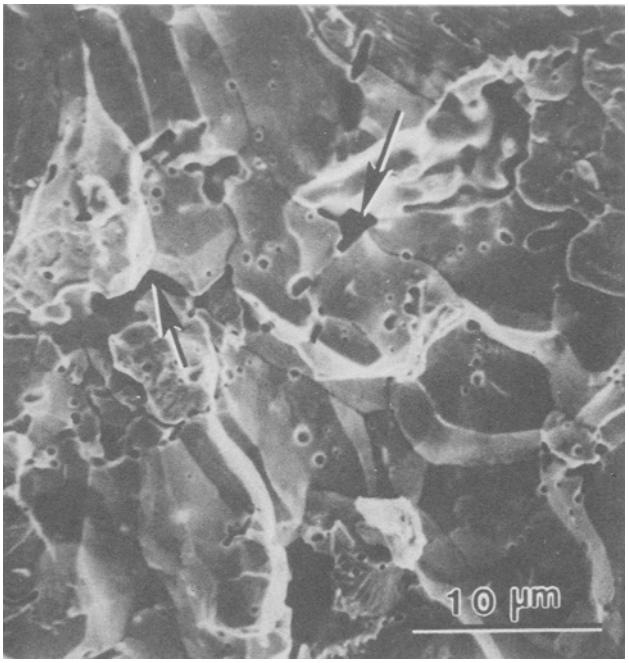

(c)

Fig. 3 Morphology of the fracture surface. (a) Both transgranular and intragranular. (b) Intragranular pores. (c) Transgranular pores

reveal the presence of any reaction products in the LPPS-processed tungsten, again suggesting that contamination is not a problem during LPPS processing.

3.3 *Porosity in LPPS-Processed Tungsten and Mechanisms of Porosity Formation*

The measured density of the deposited tungsten was 17.507 g/cm^3. Comparison of this value with the theoretical density of tungsten, 19.250 g/cm^3 (Ref 1), suggests a porosity of 9.1%. This result is consistent with SEM studies of the fracture surface, which revealed that an elevated concentration of micrometer-sized pores was present in the LPPS-processed tungsten (Fig. 3). Figure 3(a), for example, shows a fracture surface of the LPPS-processed tungsten that clearly reveals that pores were present both intragranularly and transgranularly. Small intragranular pores with an equivalent diameter that was generally smaller than 2 μm (0.1 to 2 μm) were observed on cleavage surfaces (Fig. 3b). Relatively large pores (in the range of 1 to 5 μm) were generally present on the grain boundaries (Fig. 3c).

Inspection of the available scientific literature reveals that numerous investigators have studied the effects of processing parameters on the density of plasma-processed materials (Ref 7, 11, 15, 18). For example, Smith and Mutasim (Ref 15) have studied the concomitant influences of gas flow rate, nozzle type, spray distance, and other variables on the density of the deposit. Evidently, the formation of porosity during plasma spraying and deposition is influenced by a number of factors. In the discussion that follows, the mechanisms that are thought to be responsible for the formation of porosity are discussed in terms of the following factors: the degree of melting of powders, porosity in the as-received powder, and solidification shrinkage.

The mechanisms governing the formation of porosity are thought to be related to the degree of melting of powders upon impingement with the deposition surface during plasma processing. The degree of melting during plasma spraying is primarily associated with the particle/plasma interaction (Ref 6). During plasma processing, an extremely sharp temperature gradient exists in the plasma jet. For example, the work done by McKelliget et al. (Ref 19) indicated that the temperature field varies from 1000 to 12,000 K in a plasma jet for argon/hydrogen plasma. Therefore, depending on powder type, size, shape, and injection velocity, various powder states are produced as the powders travel through this gradient. These should include fully molten powders (droplets) and partially molten powders and/or unmelted powders. Consequently, the spray may consist of fully molten, partially molten, or unmelted powders during impingement with the substrate.

Many investigators (Ref 6, 13, 18, 20) have indicated that to achieve high densities during plasma spraying, a large proportion of the powders must be completely molten during impingement with the deposition surface. Therefore, the presence of partially molten or unmelted powders normally results in a low deposit density. In the case of tungsten, there is likely to be a significant proportion of partially molten or unmelted powders because of the elevated temperature of fusion of this material. Thus, when these partially molten or unmelted powders impinge, first on the substrate and subsequently on each other, they do not deform extensively, leading to the formation of interstitial porosity. The work performed by Jackson et al. (Ref 12), for example, showed that incomplete melting of coarse tungsten powders resulted in a low deposit density, providing experimental support to this suggestion. This mechanism is thought to be responsible for the pores present on the grain boundaries (Fig. 3c).

On the other hand, another mechanism that is thought to be responsible for the formation of the porosity observed herein re-

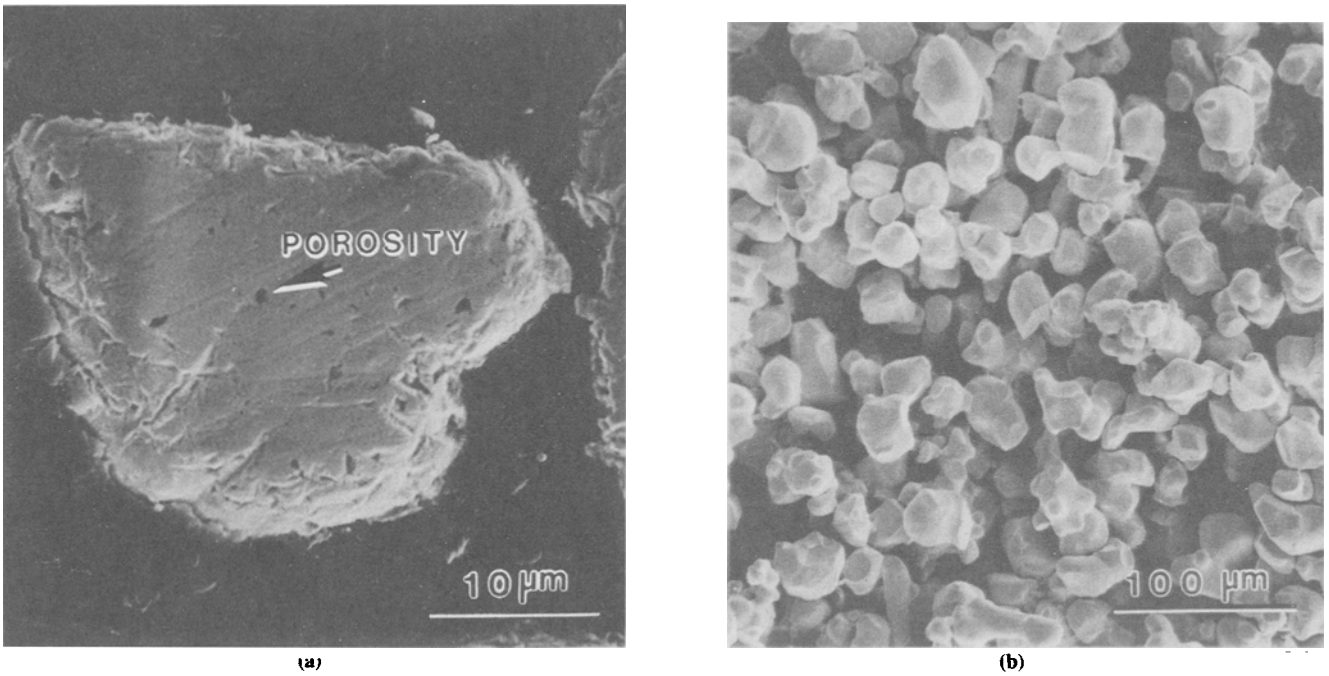

Fig. 4 Morphology of the as-received tungsten powder. (a) Internal porosity. (b) Surface morphology

sults from the interaction between the droplets and the substrate during plasma spraying. This mechanism is described as follows. A completely molten droplet, after impinging on the substrate or on other droplets, tends to spread out radially in the form of a thin disk. When the bonding between the thin disk and the contact surface below it is not sufficiently strong, however, the outer portion of the disk tends to break off or curl up at the edges and fold in toward the center (Ref 6). Hence, any cavities that are not subsequently filled by incoming droplets remain as porosity in the plasma-deposited material. In this case, the porosity produced should be relatively small, such as that present in the grain boundaries.

A third possible mechanism is based on SEM observations of the as-received tungsten powders, which revealed the presence of some pores (Fig. 4). Most of these pores appeared to be located in the interior of the powders (Fig. 4a); the surface seldom revealed any porosity (Fig. 4b). Because some of the powders were partially molten or unmelted during spraying, as discussed above, it is plausible that the porosity that was present in the as-received powders eventually became entrained in the deposited tungsten. Such pores would correspond to those observed intragranularly (i.e., inside grains), as shown in Fig. 3(b).

Finally, the presence of solidification shrinkage may also have contributed to the formation of pores during plasma processing. The fracture surface of the LPPS-processed tungsten provides experimental support to this suggestion. As shown in Fig. 5, solidification shrinkage is present as irregular cavities that form as a result of differences in the molar volumes of the solid and liquid during material solidification. Therefore, the nonuniform shrinkage during solidification of both completely molten powders and partially molten powders would certainly contribute to the porosity in the deposited materials. The pores resulting from the shrinkage mechanism may be present both intragranularly and transgranularly.

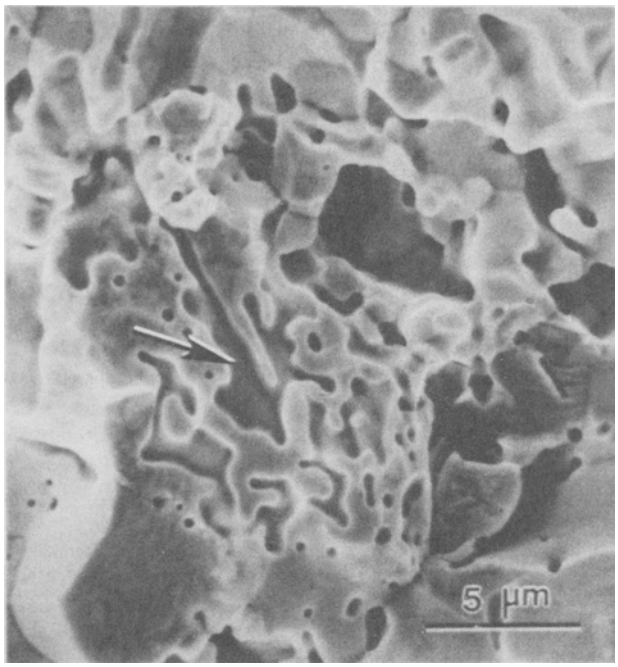

Fig. 5 Morphology of the fracture surface showing pores resulting from solidification shrinkage

In summary, the formation of porosity in the LPPS-processed tungsten can be attributed to the following factors: the presence of unmelted powders, the interaction of droplets and the substrate, the entrainment of porosity in the as-received powders, and solidification shrinkage. Therefore, decreasing the proportion of the unmelted powders during plasma spraying should significantly decrease the amount of porosity in LPPS-processed tungsten, thereby improving the quality and properties of the material. Regarding the porosity that forms from the interaction between the droplet and the deposition surface, more experimental and theoretical studies are necessary to ascertain the importance of this mechanism. To that effect, the results of a numerical analysis for the deformation and solidification of molten droplets during plasma spraying of tungsten are discussed in the next section.

3.4 *Influence of Processing Parameters on the Formation of Porosity during Plasma Spraying of Tungsten*

A numerical simulation was conducted to elucidate the influence of droplet temperature, initial impact droplet velocity, substrate temperature, and the viscosity and surface tension of the molten metal on the formation of porosity during the plasma spraying of tungsten. The corresponding model formulation is described in detail elsewhere (Ref 21, 22); hence, only a brief description is given here.

The numerical analysis was performed to simulate the deformation and solidification behavior of single and multiple tungsten droplets impinging onto a flat target surface during plasma spraying. The full Navier-Stokes equations, coupled with the volume of fluid (VOF) function, were solved to determine the exact movement and interaction of droplets. A two-domain method was employed for the treatment of the thermal field and solidification problem within the flattening droplet to track the moving solid/liquid interface. A two-phase flow continuum model was employed for the simulation of the flow problem with a growing solid layer during droplet impingement. Droplets had an initial diameter of 30 μm with impact velocities of 100, 400, or 900 m/s. Droplet temperatures of 3650 and 3750 K and substrate temperatures of 1000, 1500, 2000, 2900, and 3400 K were employed in the calculation.

The numerical results reveal that during impingement on a flat substrate, a single droplet spreads uniformly in the radial direction and eventually solidifies into a thin splat. For a low (100 m/s) or a high (900 m/s) initial impact velocity, a relatively low microporosity is generated. A low initial impact velocity, however, leads to a low degree of flattening, resulting in a small contact area with concomitant weak adhesion with the substrate and the possible formation of macropores. An initial impact velocity of 400 m/s produces a larger microporosity under the thermal conditions considered herein. Therefore, an initial impact velocity of 900 m/s or greater is preferred.

In order to reduce the formation of micropores and improve the contact and adhesion of the splat with the substrate, a substrate temperature of 3400 K, combined with a droplet temperature of 3650 or 3750 K, appears to yield optimal results; a substrate temperature of 2000 K yields the most inferior results.

For the other substrate temperatures considered in this study (2900, 1500, and 1000 K), a droplet temperature with a lower superheat is preferred.

The separation of the splat edge from the substrate or generally from the solid/liquid interface plays an important role in the formation of micropores. When the initial impact velocity or the substrate temperature is sufficiently high so that significant deformation occurs prior to extensive solidification, the separation does not take place, or occurs at a later time, and hence the resultant microporosity is low. When the initial impact velocity or the substrate temperature is sufficiently low so that extensive solidification is completed prior to significant deformation, microporosity is also relatively low. The latter phenomenon is attributed to either a reduction in the amount of void area or a reduction in total solidification time, despite the fact that the separation occurs at an earlier time for a lower substrate temperature. In this case, however, the degree of contact and eventual adhesion of the splat with the substrate may be lessened because of the small degree of flattening. When the initial impact velocity or the substrate temperature is between these two extremes, the deformation velocity and the solidification velocity become comparable, and most of the voids formed through the separation in the fringe region of the splat during deformation are fixed in the solidified layer. As a result of these conditions, the resultant microporosity is high.

Therefore, from the results of the numerical analysis, it is evident that a larger initial droplet velocity will result in a high-density deposit. The results also show that both substrate temperature and droplet temperature play important roles in the formation of porosity during plasma spraying. Thus, porosity may be effectively controlled through a suitable combination of droplet temperature, initial impact droplet velocity, and substrate temperature by adjusting the various operating parameters.

4. Conclusion

The following conclusions can be drawn:

- The microstructure of LPPS-processed tungsten exhibited an equiaxed grain morphology, with grain sizes in the range of 3 to 90 μm and an average size of 17 μm.
- The contamination of tungsten by carbon, nitrogen, and oxygen during the plasma processing was relatively insignificant.
- Pores were present both transgranularly and intragranularly, contributing to an overall porosity of 9.1%. The formation of porosity was rationalized on the basis of the following factors: the interactions between powders or droplets and the substrate, the presence of porosity in the as-received powders, and the formation of solidification shrinkage.
- According to results of the numerical simulation, a larger initial droplet velocity will result in a high-density deposit. The results also show that both substrate temperature and droplet temperature play important roles in the formation of porosity during plasma spraying. Thus, porosity may be effectively controlled through a suitable combination of droplet temperature, initial impact droplet velocity, and substrate temperature by adjusting the various operating parameters.

Acknowledgments

The authors wish to acknowledge the Army Research Office (Grant No. DAALO3-92-G-0181) and Electro-Plasma Inc. (Irvine, CA) for financial support and encouragement.

References

1. J. Shackelford and W. Alexander, *The CRC Materials Science and Engineering Handbook*, CRC Press, 1992
2. J.P. Wittenauer, T.G. Nieh, and J. Wadsworth, Tungsten and Its Alloys, *Adv. Mater. Process.*, Vol 142(No. 3), 1992, p 28-37
3. A. Belhadjhamida and R.M. German, Tungsten and Tungsten Alloys by Powder Metallurgy—A Status Review, *Tungsten and Tungsten Alloys—Recent Advances*, A. Crowson and E.S. Chen, Ed., TMS, 1991, p 3-19
4. S.W.H. Yih and C.T. Wang, *Tungsten*, Plenum Press, 1979
5. A.R. Moss and W.J. Young, The Role of Arc-Plasma in Metallurgy, *Powder Metall.*, Vol 7(No. 14), 1964, p 261-289
6. D. Apelian, M. Paliwal, R.W. Smith, and W.F. Schilling, Melting and Solidification in Plasma Spray Deposition—Phenomenological Review, *Int. Met. Rev.*, Vol 28(No. 5), 1983, p 271-294
7. D. Apelian, R.W. Smith, and D. Wei, Particle Melting and Droplet Consolidation During Low Pressure Plasma Deposition, *Powder Metall. Int.*, Vol 20(No. 2), 1988, p 7-10
8. R. Tiwari, H. Herman, S. Sampath, and B. Gudmundsson, Plasma Spray Consolidation of High Temperature Composites, *Mater. Sci. Eng.*, Vol A144, 1991, p 127-131
9. S. Sampath and H. Herman, Plasma Spray Forming Metals, Intermetallics, and Composites, *JOM*, Vol 45(No. 7), 1993, p 42-49
10. A. Sickinger and E. Muehlberger, Advanced Low Pressure Plasma Application in Powder Metallurgy, *Powder Metall. Int.*, Vol 24(No. 2), 1992, p 91-94
11. Z.Z. Mutasim and R.W. Smith, Low Pressure Plasma Spray Deposition of W-Ni-Fe Alloy, *Tungsten and Tungsten Alloys—Recent Advances*, A. Crowson and E.S. Chen, Ed., TMS, 1991, p 69-73
12. M.R. Jackson, P.A. Siemers, S.F. Rutkowsky, and G. Frind, Refractory Metal Structures Produced by Low-Pressure Plasma Deposition, *Int. J. Refract. Hard Met.*, Vol 8(No. 3), 1989, p 196-200
13. R.W. Smith and D. Apelian, Plasma Spray Consolidation of Materials, *Pure Appl. Chem.*, Vol 62(No. 9), 1990, p 1825-1832
14. C.N.R. Rao, M.V. George, J. Mahanty, and P.T. Narasimhan, *Handbook of Chemistry and Physics*, Van Nostrand-Reinhold, London, 1970
15. R.W. Smith and Z.Z. Mutasim, Plasma Sprayed Refractory Metal Structures and Properties, *Thermal Spray Research and Applications*, T.F. Bernecki, Ed., ASM International, 1991, p 369-374
16. J.A. Shields, Jr., The Processing and Joining of High-Temperature Materials, *JOM*, Vol 45(No. 6), 1993, p 48
17. P.T.B. Shaffer, *Plenum Press Handbooks of High-Temperature Materials, No. 1—Materials Index*, Plenum Press, 1964
18. H. Gruner, Vacuum Plasma Spray Quality Control, *Thin Solid Films*, Vol 118(No. 4), 1984, p 409-420
19. J. McKelliget, J. Szekely, M. Vardelle, and P. Fauchais, Temperature and Velocity Fields in a Gas Stream Exiting a Plasma Torch. A Mathematical Model and Its Experimental Verification, *Plasma Chem. Plasma Process.*, Vol 2(No. 3), 1982, p 317-332
20. B. Champagne and S. Dallaire, Particle Injection in Plasma Spraying, *Thermal Spray: Advances in Coating Technology*, D.L. Houck, Ed., ASM International, 1988, p 25-32

21. H. Liu, E.J. Lavernia, and R.H. Rangel, Numerical Simulation of Substrate Impact and Freezing of Droplets in Plasma Spray Processes, *J. Phys. D, Appl. Phys.*, Vol 26(No. 11), 1993, p 1900-1908

22. H. Liu, E.J. Lavernia, and R.H. Rangel, Numerical Investigation of Micro-Pore Formation During Substrate Impact of Molten Droplets in Plasma Spray Processes, *Atomiz. Sprays*, in press, 1994